Cerebral Cortex December 2008;18:2909–2919
doi:10.1093/cercor/bhn051
Advance Access publication April 15, 2008

Members of the NuRD Chromatin Remodeling Complex Interact with AUF1 in Developing Cortical Neurons

Cheol Lee[1,2], Andrea Gyorgy[2], Dragan Maric[3], Navid Sadri[4], Robert J. Schneider[4], Jeffery L. Barker[3], Michael Lawson[2] and Denes V. Agoston[1,2]

[1]Neuroscience Program, [2]Department of Anatomy, Physiology and Genetics, School of Medicine, USUHS, Bethesda, MD 20814, USA, [3]Laboratory of Neurophysiology, NINDS, NIH, Bethesda, MD 20892, USA and [4]Department of Microbiology, New York University School of Medicine, New York, NY 10016, USA

Cheol Lee and Andrea Gyorgy contributed equally to this work.

Chromatin remodeling plays an important role in coordinating gene expression during cortical development, however the identity of molecular complexes present in differentiating cortical neurons that mediate the process remains poorly understood. The A + U–rich element-binding factor 1 (AUF1) is a known regulator of messenger RNA stability and also acts as a transcription factor upon binding to AT-rich DNA elements. Here we show that AUF1 is specifically expressed in subsets of proliferating neural precursors and differentiating postmitotic neurons of the developing cerebral cortex. Moreover, AUF1 is coexpressed with histone deacetylase 1 (HDAC1) and metastasis-associated protein 2 (MTA2), members of the nucleosome remodeling and histone deacetylase complex. AUF1 specifically and simultaneously binds to HDAC1, MTA2, and AT-rich DNA element, its gene regulatory function is modulated by the extent of histone acetylation and in animals lacking AUF1, the composition of the complex is modified. These results suggest that AUF1 is involved in integrating genetic and epigenetic signals during cortical development through recruiting HDAC1 and MTA2 to AT-rich DNA elements.

Keywords: cerebral cortex, epigenetics, gene expression, histone acetylation, neuronal differentiation, progenitors

Introduction

Normal cortical development is influenced by both genetic and epigenetic factors resulting in a precisely coordinated expression of genes in differentiating neurons. It has been shown that chromatin remodeling can play a significant role in corticogenesis (Berube et al. 2005, however, the full identity of molecules required for the developmental process is currently not known (Hsieh and Gage 2005). During our search for DNA-binding proteins that are specifically expressed in the developing brain we found A + U–rich element-binding factor 1 (AUF1) (Dobi et al. 2006). Although we isolated AUF1 (also called hnRNPD; Dempsey et al. 1998) based on its ability to bind AT-rich double-stranded DNA (dsDNA), AUF1 was originally identified as an AU-rich element-binding protein (Zhang et al. 1993 Brewer 2002; Lu et al. 2006). Alternative splicing of exon2 and exon7 of the AUF1 primary transcript results in 4 isoforms, p37 (A), p40 (B), p42 (C), and p45 (D) (Wagner et al. 1998; Wilson and Brewer 1999; Laroia and Schneider 2002. AUF1 proteins are found both in the cytoplasm and also in the nucleus depending on the cell and tissue type (Blaxall et al. 2000 Sarkar et al. 2003) and they can perform various molecular regulatory functions. The p37 isoform has been shown to regulate messenger RNA (mRNA) stability (Sarkar et al. 2003), we showed that it also binds AT-rich dsDNA with high specificity and acts as a transcriptional regulator (Dobi et al. 2006). In addition, studies using various cell culture and in vitro models showed that the p40 isoform interacts with the TATA binding protein and regulates gene expression (Tolnay et al. 2000). The p42 isoform binds single-stranded telomeric C-strand, interacts with telomerase and is involved in regulating telomeric length (Eversole and Maizels 2000; Enokizono et al. 2005.

Our initial study showed high levels of AUF1 expression in the embryonic cortex, suggesting that AUF1 proteins may be involved in regulating corticogenesis (Dobi et al. 2006). As a 1st step toward understanding the molecular function of AUF1 in the developmental process, we set out to determine the phenotype of AUF1+ cells in the embryonic rat brain. Because we found that the spatial and temporal pattern of AUF1 expression (Dobi et al. 2006) and histone deacetylase 1 (HDAC1) and metastasis-associated protein 2 (MTA2), members of the nucleosome remodeling and histone deacetylase (NuRD) chromatin remodeling complex (Szemes et al. 2006), are remarkably similar in the developing rat brain, we designed experiments to determine if AUF1, HDAC1, and MTA2 are coexpressed and interact in developing cortical neurons. Lastly, we set out to determine the functional significance of the detected interactions by analyzing the effect of altered histone acetylation on the regulatory function of AUF1 using a primary embryonic cell culture model. Our results suggest that AUF1 is involved in coordinating gene expression of proliferating neural precursors/progenitors and postmitotic neurons of the cerebral cortex through recruiting chromatin remodeling molecules to AT-rich DNA elements.

Materials and Methods

Animals

Timed-pregnant Sprague–Dawley rats (Zivic Laboratories, Inc., Pittsburgh, PA) were used in these studies. All animals were treated in accordance with institutional and National Institutes of Health guidelines for the Care and Use of Laboratory Animals. Animal protocols were approved by the Institutional Animal Care and Use Committee at Uniformed Services University of the Health Sciences (USUHS).

Tissue Preparation

Following Ketamine/Xylazine anesthesia, rat embryos were obtained from timed pregnancies, and their brains were removed and fixed by immersion in 4% paraformaldehyde (PF). Fixed brains were cryoprotected by immersing them in cold 15% and 30% sucrose solution in phosphate buffered saline (PBS). Frozen brains were cut coronally in 20-μm sections with a cryostat (Cryocut 1800, Leica, Bannockburn, IL). Sections were mounted on Colorfrost plus slides (Fisher Scientific, Suwanee, GA) and kept at –80 °C until use.

Flow Cytometric Analysis

Fluorescence-activated cell sorting (FACS) analysis was performed as described previously (Maric et al. 2003. Briefly, telencephalic tissues

from E13 and E19 rat embryos were dissociated into single cell suspensions and cells were immunophenotyped using cell surface markers, tetanus toxin fragment C and A2B5. The cells were then fixed in 4% PF and subsequently labeled using anti-proliferating cell nuclear antigen (PCNA) and anti-AUF1 antibodies. The cells were enumerated and their immunoreactions quantified using the FACSVantage SE flow cytometer and Cell Quest Acquisition and Analysis software (Becton Dickinson, Mountain View, CA), as previously described (Maric et al. 2003).

Immunohistochemistry

Immunohistochemistry was performed as described earlier (Szemes et al. 2006) using the following primary antibodies: AUF1 (1:500) (Lu and Schneider 2004); Phospho-Histone H3 (PH3) (1:100, Cell Signaling Technology, Danvers, MA); nestin (1:1000, Chemicon, Temecular, CA); TuJ1 (1:1000, Babco, Berkeley, CA); HDAC1 (1:50, Upstate, Charlottesville, VA); and MTA2 (1:200, Abcam, Cambridge, MA). For double immunohistochemistry, Zenon Rabbit IgG Labeling Kit was used according to the manufacturer's instructions (Invitrogen, Carlsbad, CA). Primary antibodies were visualized with the following secondary antibodies: Alexa Fluor 555 goat anti-mouse IgG (1:5000) and Alexa Fluor 488 goat anti-rabbit IgG (1:5000) (both from Invitrogen). Nuclei were counterstained using Hoechst 33342 (Molecular Probes, 1 μg/mL applied for 2 min). Sections were analyzed in an Olympus IX71 microscope equipped with a Spot camera (Diagnostic Instruments, Sterling Heights, MI). In order to assess the extent of coexpression, images were captured using a Zeiss Pascal Laser Scanning Confocal Microscope. The parameters of image acquisition (including laser power, detector gain, offset, etc.) were preset to maximize signal and minimize background and were kept constant (Gyorgy 2006; Gyorgy, unpublished data. We assessed the extent of AUF1 and MTA2 or AUF1 and HDAC1 coexpressions by counting red and green pixels of TIFF images using a Mathematica 5.2 script (Wolfram Research, Inc. software, Urbana, IL; script written by Dr J. Czege, Biomedical Instrumentation Center, USUHS). The script is freely available at http://bic.usuhs.mil/agoston/quantification.html. The script counts every pixel that has either a green and/or red value above the background threshold. The number of red, green and yellow (green + red) pixels, indicating coexpression, were counted and expressed as the ratio of pixels over the total numbers of colored pixels above the set threshold. Identical cortical regions of 4 independent double staining experiments were analyzed.

Western Blot

Embryonic and neonatal rat whole brains were microdissected under a stereomicroscope and tissues were snap-frozen in liquid nitrogen and stored at –80 °C until used. The isolation of nuclear and soluble proteins, electrophoresis and transfer were described earlier (Dobi et al. 2006; Szemes et al. 2006). Twenty micrograms of proteins were loaded and separated as described. Transferred proteins were probed with AUF1 antibody as described (Dobi et al. 2006) or commercial AUF1 antibody (Upstate Biotechnology, Waltham, MA) both diluted at 1:1000. Immunoreactive bands were visualized using the SuperSignal enhanced chemiluminescence detection system (Pierce, Rockford, IL) and quantified using a Fuji LAS-1000 CCD Camera and the Fuji Image Gauge software (Fuji Photo Film USA, Valhalla, NY).

Coimmunoprecipitation Assay

Nuclear and cytoplasmic proteins were prepared as described (Dobi et al. 2006; Szemes et al. 2006). Proteins were dialyzed against buffer D (20% glycerol, 20 mM 4-(2-hydroxyethyl)-1-piperazineethanesulfonic acid (HEPES) (pH = 7.9), 100 mM KCl, 0.2 mM EDTA 0.5 mM dithiotreitol [DTT], 0.5 mM AEBSF) for 2 h, changing the buffer after 50 min, at 4 °C, in the 3500 MWCO Slyde-A-Lyzer Mini Dialysis Unit (Pierce, Rockford, IL). For preclearing, 50 μg of nuclear extracts were incubated with 50 μL of the Protein A Sepharose bead slurry in 400 μL total volume under constant, slow rotation for 1 h at 4 °C, then sedimented by centrifugation for 10 min at 10 000 *g*, also at 4 °C. The precleared nuclear extracts were then immunoprecipitated with 2 μg of anti-AUF1 antibody or with 2 μg of control antibody (EGFR, Santa Cruz Biotechnology, Inc., Santa Cruz, CA) for 2 h. Immunocomplexes were captured by adding 100 μL of the Protein A Sepharose bead slurry. After 1 additional hour of rotation at 4 °C the bound fraction was separated by pulse centrifugation. The beads were washed 3 times with 1 mL of ice-cold washing buffer (1× PBS containing 0.1% Igepal). After the last wash, beads were resuspended in 2× loading buffer containing 0.1 M DTT and LDS (lithium dodecyl sulfate) sample buffer (Invitrogen, Carlsbad, CA) denatured at 80 °C for 10 min, centrifuged at 10 000 *g* for 5 min at room temperature, and processed for Western analysis as described above.

DNA Affinity Preincubation Specificity Test of Recognition assay

The DNA affinity preincubation specificity test of recognition (DAPSTER) assay was performed as described earlier (Kumar and Bernstein 2001) and optimized for the developing brain (Dobi et al. 2006). Nuclear proteins were precleared with a streptavidin agarose bead slurry (ImmunoPure Immobilized Streptavidin, Pierce) without DNA. One hundred and fifty micrograms of the precleared nuclear extracts were preincubated with Poly (2′-deoxyinosinic-2′-deoxycytidylic acid) 6 μg/mL for 10 min on ice followed by the addition of either 600 pmol of specific competitor ds rAT (5′rAT annealed with 3′rAT, for sequence information see Table 1) or 600 pmol of control competitor dsDNA (5′ rAT_{Mut} annealed with 3′ rAT_{Mut}) or kinase buffer only. Biotinylated AT-rich DNA probes (5′Bio-rAT) were annealed and 150 pmol of the dsBio-rAT was coupled to streptavidin beads, then washed with buffer Z (25 mM HEPES pH 7.9, 20% glycerol, 0.1% Igepal, 0.1 M KCl, 12.5 mM $MgCl_2$, 1 mM DTT, 0.1 μM $ZnCl_2$). Samples and beads containing the various immobilized DNA probes were mixed and incubated for an additional 2 h at 4 °C. Bound fractions were then separated by pulse centrifugation and beads were washed 3 times with 1 mL of ice-cold buffer *Z* each. Beads were resuspended in 2× LDS loading buffer, proteins denatured by boiling and samples were analyzed by Western blot as described above.

Chromatin Immunoprecipitation

The assay was performed using the EZ-ChIP Kit from Upstate (Charlottesville, VA) according to the manufacturer's instructions, and optimized to neonatal rodent brain tissue. All buffers used were supplemented with protease inhibitors. Briefly, snap-frozen whole brain tissue pieces from P2 wild-type and AUF1 mutant mice were transferred into 5 mL of 1× PBS containing 1% formaldehyde and rotated for 15 min on room temperature. Cross-linking reactions were stopped by the addition of 500 μL of 10× Glycine Buffer, then washed twice with 1× PBS, and finally the cross-linked tissue was lysed with lysis buffer. Cells were disrupted by sonication on ice (6, 10-s long bursts at tune 4, setting no. 6, each run separated by 60-s cooling breaks). After centrifugation, supernatants were aliquoted, then diluted with Dilution Buffer. Next, the samples were precleared in the presence of DNA- and bovine serum albumin–blocked, protein A–coupled agarose beads for 60 min on 4 °C. The precleared supernatants were then incubated overnight at 4 °C with 5 μg of 1 of the following antibodies: AUF1 (Upstate), HDAC1 (Upstate), MTA2 (Abcam), SATB2 (Szemes et al. 2006), or normal rabbit serum as a negative control. One aliquot was not immunoprecipitated and was later used as the input control sample. Then 60 μL of DNA- and bovine serum albumin–blocked, protein A–coupled agarose beads were added to each sample. The samples were then incubated under constant rotation overnight at 4 °C. The precipitated samples were washed once

Table 1
Sequence information for Oligonucleotides used in the DAPSTER assay

Name	Sequence 5′–3′
5′rAT	GAA CCA AAA ATA ATA ATA ATA ATA ATA ATA ATA ATA ATA ATA ATA ATA ATA ATT AAC CAT
3′rAT	ATG GTT AAT TAT TAT TAT TAT TAT TAT TAT TAT TAT TAT TAT TAT TAT TAT TAT TAT TAT TTT TGG TTC
5′rAT_{Mut}	GAA CTG TTC TTA CTA TCG CCA TCA CCG TTA TTG CTC AAT TCG TAC TAG TTC ATG AAG TCT TTG G
3′rAT_{mut}	CCA AAG ACT TCA TGA ACT AGT ACG AAT TGA GCA ATA ACG GTG ATG GCG ATA GTA AGA ACA GTT C

with 1 mL of low salt buffer, once with high salt buffer, once with the LiCl buffer, and twice with room temperature 1× Tris-EDTA buffer. After the final wash, the precipitated protein–DNA complexes were eluted by the addition of elution buffer containing 0.5% sodium dodecyl sulfate and 0.1 M $NaHCO_3$, and after incubating for 30 min on room temperature, the supernatants were supplemented with NaCl to and end concentration of 0.3 M, and incubated overnight at 65 °C to reverse the cross-linking. Proteins and RNA were removed by the addition of ProteinaseK and RnaseH. The precipitated genomic DNA was purified using the QiaQuick PCR purification kit (Qiagen, Valencia, CA). Three microliters of the purified DNA was used as a template in the 1st PCR; for the input sample, the DNA was diluted 100 times.

For the rat samples, the rENK2700-703-LUC plasmid containing the rat AT-rich DNA element was used as a positive control. Here, the 1st PCR was carried out using 25 cycles, with primers specific to the rAT region: 5′tAT-O and 3′rAT-O (Table 2) After the 1st PCR, amplicons were diluted 100 fold and used as templates in the 2nd (nested) PCR reaction using 25 cycles with primers 5′rAT-N and 3′rAT-N. In the negative control, no DNA template was used, but an equal amount of PCR-grade water was instead added to the mix. The PCR products were separated on 2.5% agarose gel along with a 100-bp molecular weight ladder. Bands were visualized with ethidium bromide.

For the mouse samples, primers were designed to allow quantification of the products. Accordingly, all oligonucleotides were 24 mers, with a GC content of 50% (±4) and a Tm of 60 °C (±2.0), keeping the product size between 250 and 700 bp (Strahl-Bolsinger et al. 1997). The 1st PCR was carried out using 25 cycles, with primers specific to the mouse AT region: 5′mAT-O and 3′mAT-O (Table 2). After the 1st PCR, amplicons were diluted 10-fold and used as templates in the 2nd (nested) PCR using 25 cycles with primers 5′mAT-N and 3′mAT-N. Glyceraldehyde 3-phosphate dehydrogenase (GAPDH) as used as a negative control gene, and was amplified with 5′GAPDH and 3′GAPDH primers from samples precipitated with SATB2, AUF1, MTA2 antibodies. The PCR products were separated on 1.5% agarose gel along with a 100-bp molecular weight ladder, and bands were visualized with SYBR-Green. The bands were visualized on a FUJI 3000 LAS intelligent dark box equipped with a CCD camera, and the band densities quantified using the ImageGouge software.

Cell Cultures and Transfection

Mouse embryonic fibroblast (MEF) cells were obtained from AUF1 mutant and wild-type animals (Lu et al. 2006). MEF-$AUF1^{-/-}$ and MEF-$AUF1^{+/+}$ cells were cultured in DMEM in the presence of 2 mM l-glutamine and 10% heat-inactivated fetal calf serum. The AT-rich DNA element was inserted in the plasmid pTK-Renila (Promega, Madison, WI) resulting the reporter plasmid pTK-rAT-Ren in which the baseline activity of Renila luciferase is modified by AUF1 proteins (Dobi et al. 2006; Szemes et al. 2006). In the control reporter plasmid TK-rAT_{mut}-Ren the AT-rich DNA element was mutated so the resulting sequence failed to bind AUF1 (Dobi et al. 2006). Cells were transfected using the PEI transfection system as previously described (Szemes et al. 2006) with 1.5 μg of the reporter plasmids (TK-rAT-Ren or TK-rAT_{mut}-Ren) and 0.1 μg of rous sarcoma virus (RSV)-Firefly Luciferase Promega, Madison, WI) enabling normalization for transfection efficiency. Forty-eight hours after transfection, some of the cultures were treated with 1 mg/mL of trichostatin A (TSA), a blocker of histone deacetylases dissolved in ethanol. Control cultures received equal volume of vehicle only. After 18 h of treatment, cultures were harvested and Firefly and Renila luciferase activities were measured using the Dual-Luciferase Assay System according to the manufacturer's instructions (Promega, Madison, WI). Relative light units (RLU) of Renila Firefly luciferase activities were normalized by Firefly RLUs representing the activities of the control plasmid (RSV-Firefly Luciferase), as recommended by the manufacturer (Promega, Madison, WI).

Table 2
Sequence information and physical characteristics of oligonucleotides used in the Chromatin Immunoprecipitation (ChIP) assay

Name	Sequence (5′–3′)	Product size	GC%	Length (nt)	Tm (°C)
5′mAT-O	ACT CGT GTT AGC CTC TGA GCT AGT	550	50	24	60.15
3′mAT-O	GTG ACA CTA GCA GAC CAG ATT CCT	550	50	24	61.08
5′mAT-N	GCC TCT GAG CTA GTA TGT GTC ATC	274	50	24	59.46
3′mAT-N	CCA TCA CCT TCT CCT TTC TAG GTC	274	50	24	61.64
5′rAT-O	TTT AGC TCA GTG GTA GAG CGC	257	52	21	56
3′rAT-O	GTT TCT GCC CTT TCC AAC TGC	257	52	21	56
5′rAT-N	CCC TGG GTT CGG TCC CCA GC	131	75	20	58
3′rAT-N	GTT CCC AGA CCT GTC CAG TTC	131	57	21	53
5′GAPDH	ATC ACT GCC ACC CAG AAG ACT G	623	67	22	60
3′GAPDH	CCC TGT TGC TGT AGC CGT ATT C	623	65	22	61

Results

AUF1 Expression is Developmentally Regulated in the Rat Brain

We determined the relative abundance of AUF1 proteins in tissue extracts prepared from E14, E15, E16, E18, P2, and P28 brains by Western blotting using pan-specific AUF1 antibodies that recognize all isoforms in an unbiased fashion (Lu and Schneider 2004). Semiquantitative assessment of band intensities showed that the level of expression of AUF1 proteins did not substantially change from E14 to P2 (Fig. 1). The commercial antibody also reacted with a ~35-kDa protein marked with star (see Supplementary Fig. 1). During development, AUF1 protein levels steadily declined and after birth (P2) the abundance of AUF1 proteins was ~30% of the E14 brain. Although AUF1 proteins can be detected in the P28 brain, their abundance was substantially lower than in the developing brain. Western analysis also showed that all AUF1 isoforms were expressed at all ages tested and that the ratio between the different isoforms was practically identical throughout development (E14 to P2). Of the various isoforms, p40/42 were the most abundant. Although the abundance of AUF1 proteins in the adult brain was very low as compared with the developing brain, it appears that the ratio between the isoforms in the adult brain was similar to that detected in the developing brain.

AUF1 is Expressed by Proliferating Precursors/ Progenitors and Postmitotic Differentiating Neurons in the Cerebral Cortex

The high level of AUF1 expression in the E14 brain suggested that AUF1 was expressed in proliferating progenitor cells that were the most abundant cell type at this developmental stage (Ohnuma and Harris 2003). We 1st carried out quantitative FACS analysis using a previously established immunophenotyping paradigm (Maric et al. 2003) to test the proliferative status of AUF1+ cells. We isolated cells from E13 telencephalon at the beginning of cortical neurogenesis, when the majority of neural precursor cells were proliferating and from E19 cortex at the end of cortical neurogenesis, when most of the neuronal cells were postmitotic. At both developmental stages, we quantified

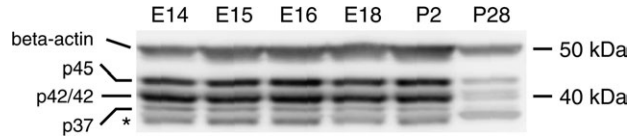

Figure 1. Expression of AUF1 proteins in the developing and adult rat brain. Representative Western blot analysis showing the relative abundance of the various isoforms at the selected ages. Star indicates the nonspecific band recognized by the anti-AUF1 antibody.

the numbers of AUF1+, PCNA+, and double-positive cells. We found that at E13 approximately 70% of the total neural precursor population was positive for both PCNA and AUF1 indicating that the large majority of AUF1-expressing cells were proliferating (Fig. 2*A*,*C* and Supplementary Fig. 2*A*,*B*). In contrast, only ~3% of the total neural precursor population was PCNA+/AUF1+ at E19. The majority (~60%) of these cells were PCNA–/AUF1+, indicating that AUF1 was widely expressed in the postmitotic/differentiating compartment of the cortical neuronal precursor cell population at this stage of cortical development (Fig. 2*B*,*C*).

We performed immunohistochemical analysis to identify the developmental phenotype of AUF1+ cells in the embryonic and early postnatal cortex. Consistent with our FACS data, during early brain development (E14) most of AUF1+ cells were located in the ventricular zone (VZ) and in the subventricular zone (SVZ), the site of proliferating precursors/progenitors (Fig. 3*A*). Double immunohistochemistry using AUF1 antibody and an antibody raised against PH3, a marker of proliferating cells in the M phase of cell cycle (Brenner et al. 2003; Rayzman and Sentry 2006 showed that virtually all PH3+ cells in the VZ also expressed AUF1 (Fig. 3*B*,*C*). Consistent with the data obtained from FACS analysis, our double immunohistochemistry using AUF1 and nestin antibodies (Kim et al. 2003) showed that at E14 the majority of AUF1+ cells expressed nestin (Fig. 3*D*–*F*) suggesting that during early brain development AUF1 was expressed by neural precursor/progenitor cells. In addition to the VZ and SVZ, we found AUF1+ cells located in the telencephalic wall (Fig. 3*A*,*D*), suggesting that AUF1 was also expressed in differentiating cortical neurons. Indeed, at E18 AUF1+ cells were located almost exclusively in the differentiating region of the cortex, especially in the cortical plate (CP) and in the marginal zone (MZ) (Fig. 3*G*). The majority of these AUF1+ cells also expressed TuJ1, a marker of postmitotic, differentiating neurons (Fig. 3*H*,*I*). In the P2 brain, the number of AUF1+ cells was substantially decreased (Fig. 3*J*). AUF1+ cells were present in all layers, however, layer I contained the fewest, whereas layer II (MZ) contained relatively higher numbers of immunoreactive cells. Practically all AUF1+ cells were also positive for MAP2 (Fig. 3*K*,*L*), indicating that in the postnatal brain, AUF1-expressing cells were postmitotic differentiating neurons. In summary, our FACS and immunohistochemistry data suggest that AUF1 was expressed by proliferating neural precursors as well as by postmitotic, differentiating cortical neurons. We found that other brain regions were mostly devoid of AUF1+ cells with the exception of the pallidal SVZ, which contained some AUF1+ cells, as we also reported earlier (Dobi et al. 2006).

AUF1 is Coexpressed and Interacts with HDAC1 and MTA2 in Developing Neurons of the Cerebral Cortex In Vitro and In Vivo

Because the spatial and temporal patterns of expression of HDAC1 and MTA2 in the developing cortex (Gyorgy 2008; Gyorgy, unpublished data appeared to be very similar to the pattern of AUF1 expression shown above, we analyzed the pattern of coexpression by immunohistochemistry in E14, E18, and P2 brains. We found that in the developing cortex, AUF1 was coexpressed with both HDAC1 and MTA2 at all ages tested. In the E14 brain, semiquantitative assessment showed that ~85% of AUF1+ cells expressed HDAC1 and ~95% of them expressed MTA2 (Fig. 4*B*,*C*). At E18 ~70% of AUF1+ cells in the CP and in the MZ coexpressed HDAC1 and ~80% of AUF1+ cells expressed MTA2. The extent of coexpression in the P2 cortex was similar to that of observed in the E18 cortex and semiquantitative assessment of coexpression also indicated that ~80% of AUF1+ cells expressed HDAC1 and also MTA2. Interestingly, differentiating cells in other major brain regions such as the thalamus that lack AUF1 expression were also negative for HDAC1 and MTA2. Higher power confocal microscopy confirmed the nuclear coexpression of all 3 proteins at all developmental ages investigated (Supplementary Fig. 3).

As a 1st test toward understanding the potential functional significance of the coexpression of AUF1 with the selected chromatin remodeling molecules, we performed a coimmunoprecipitation assay using nuclear extracts prepared from E18 cortex. Following incubation with the AUF1 antibody, we analyzed the immunoprecipitated fractions for the presence of HDAC1 and MTA2 by Western blotting. The analysis showed

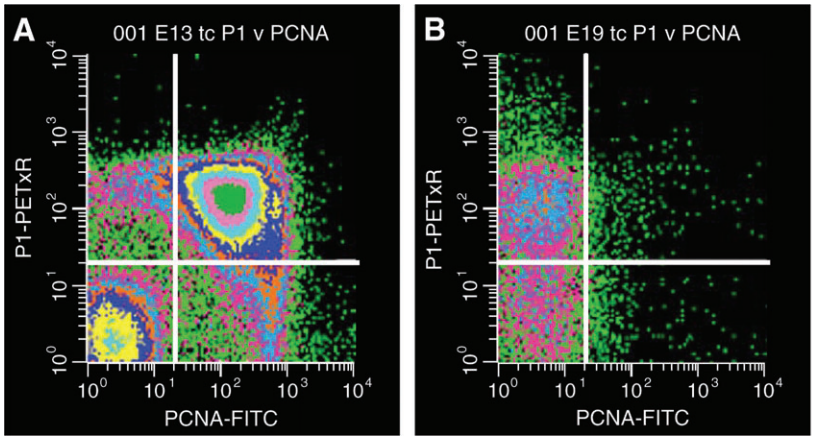

C

PCNA vs. AUF1

	E13 (%)	E19 (%)
UL	3.72	60.49
UR	71.10	3.11
LL	19.59	33.25
LR	5.59	3.16

Figure 2. The proliferative state of AUF1-expressing cells in the rat brain. The bivariate dot density plot derived from FACS analysis shows the expression(s) of PCNA and AUF1 in the mostly proliferating neural precursor/progenitor population isolated from the E13 rat telencephalon (*A*) and their predominantly postmitotic/differentiating counterparts isolated from E19 rat cortex (*B*). Cell population in the upper right quadrant represents the contribution of proliferating AUF1+ cells to the total cell population at the 2 developmental ages. The developmental changes in the percentage distribution among the various cell populations are tabulated (*C*). Upper-left (UL) represents $AUF1^{+}/PCNA^{-}$, upper-right (UR) represents $AUF1^{+}/PCNA^{+}$, lower-left (LL) represents $AUF1^{-}/PCNA^{-}$, and lower-right (LR) represents $AUF1^{-}/PCNA^{+}$ fraction, respectively.

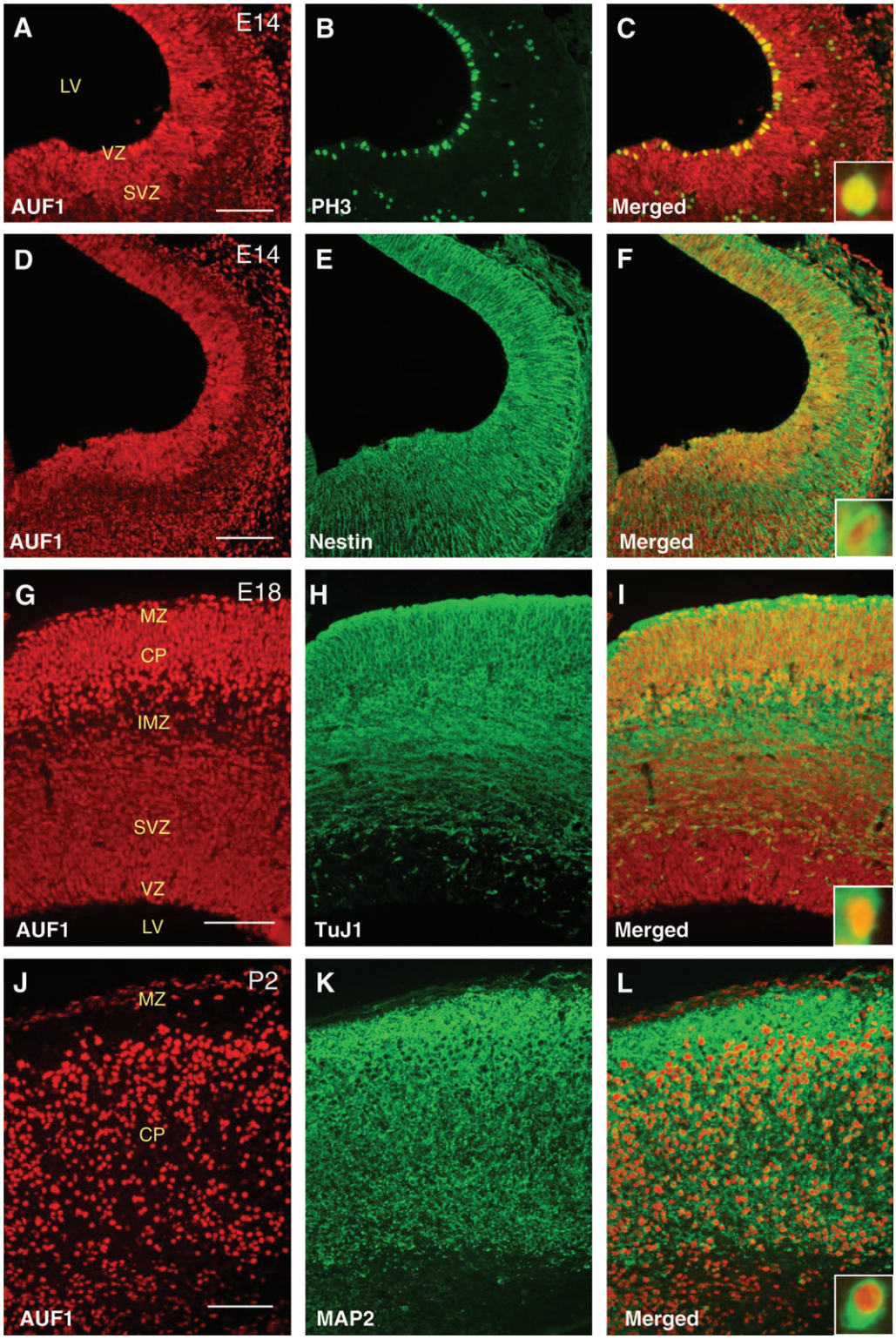

Figure 3. The developmental phenotype of AUF1-expressing cells in the rat brain. Double immunohistochemistry (*A–C*) of E14 rat coronal sections show the location of proliferating Phospho-Histone H3+/AUF1+ cells. At this age, most nestin+ cells that are located in the VZ and SVZ express AUF1 (*D–F*). At E18, most AUF1+ cells that are located in the MZ and CP of the developing cortex express TuJ1 (*G–I*). After birth, the number of AUF1+ cells decreases substantially and the remaining AUF1+ cells express MAP2 (*J–L*) at P2. LV = lateral ventricle; IMZ = intermediate zone. Scale bars in (*A–F*) = 200 μm and in (*G–L*) = 100 μm.

that both HDAC1 and MTA2 interacted with AUF1 as indicated by the presence of ~80- and ~60-KDa bands (Fig. 5*A*). We also detected an additional band at ~78 KDa, which may be a proteolytic product of MTA2, because the antibody should not cross-react with MTA1 according to the manufacturer (Abcam). We did not detect either of the proteins when we replaced the AUF1 antibody with the control antibody suggesting that both HDAC1 and MTA2 specifically bind to

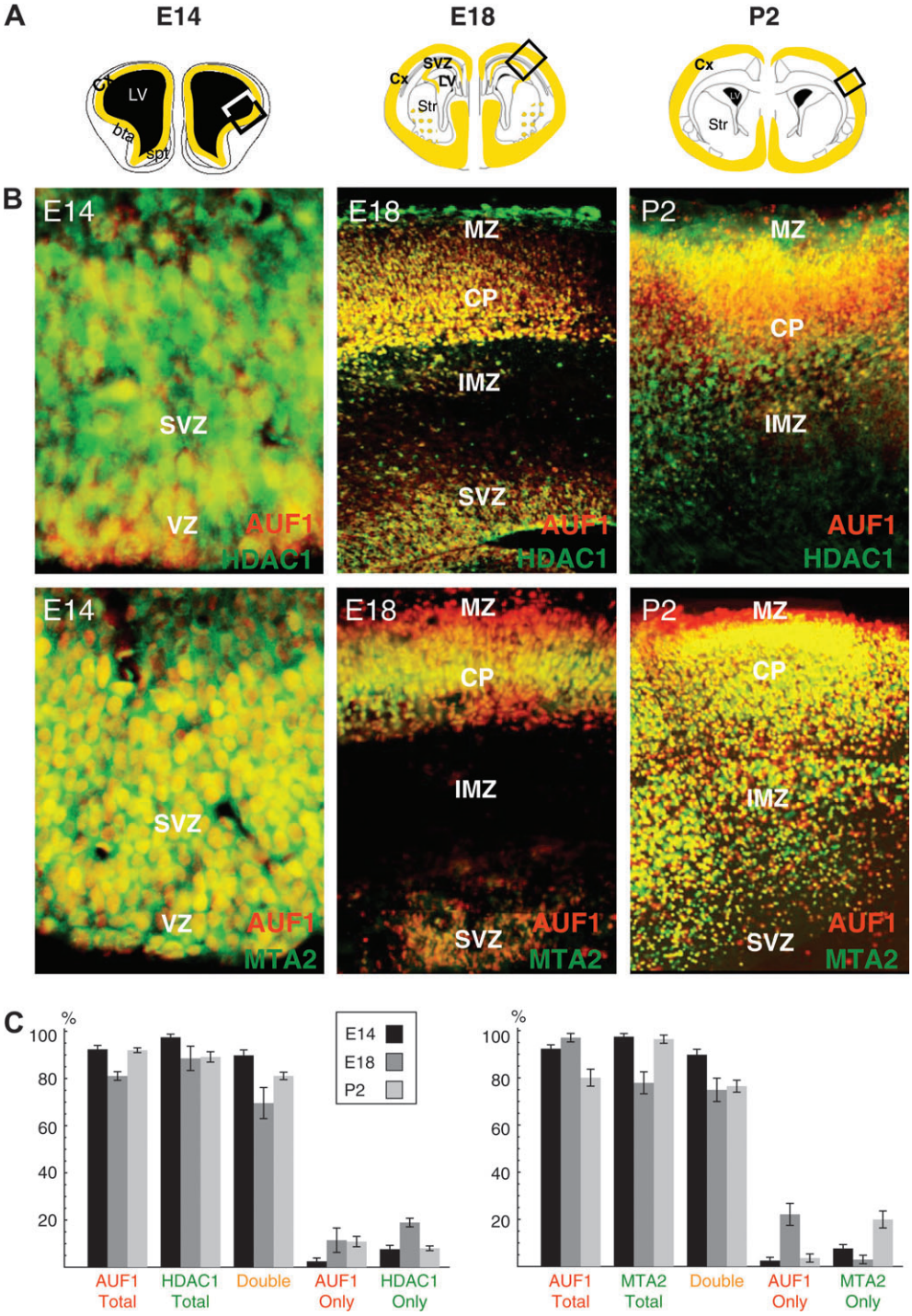

Figure 4. Pattern of coexpression of AUF1, HDAC1, and MTA2 in the developing rat brain. Anatomical maps of coronal sections of the developing rat brain at ages E14, E18, and P2 (*A*) summarizing the patterns of coexpression (yellow colored areas). Left hemispheres: AUF1/HDAC1; right hemispheres: AUF1/MTA2. Abbreviations: Bta = Basal telencephalon; Spt = septal neuroepithelium; Lv = lateral ventricle; Str = striatum; Cx = cortex. Representative double-immunohistochemical images showing the pattern of AUF1, HDAC1, and MTA2 expression in the developing rat brain (*B*). Coronal sections from E14, E18 and P2 rat brains were immunostained using a combination of AUF1 and HDAC1 (upper row) and AUF1 and MTA2 (lower row) antibodies. Abbreviations: Cx, cortex; LV, lateral ventricle; IMZ, intermediate zone. Scale bar = 1 mm. Graphs showing the extent of coexpression (AUF1/HDAC1 and AUF1/MTA2) from E14 to P2 in the developing rat cortex. The bar graphs show the ratio of red (AUF1), green (HDAC1 or MTA2), and yellow (double-positive) areas expressed as percentage of the total area scanned (*C*). Vertical axis = percentage of total color pixels. $N = 4$.

AUF1 in vitro. In the reverse immunoprecipitation experiment, HDAC1 antibody also coprecipitated AUF1 as well as MTA2 (Supplementary Fig. 4).

We 1st identified and isolated AUF1 in the developing cortex based on its specific binding to AT-rich dsDNA elements (Dobi et al. 2006). Because AUF1 was coexpressed with, and binds to HDAC1 and MTA2, we hypothesized that the molecular function of AUF1 includes recruiting HDAC1 and MTA2 to AT-rich DNA regions. To test this hypothesis, we performed a DAPSTER, a microscale DNA affinity purification

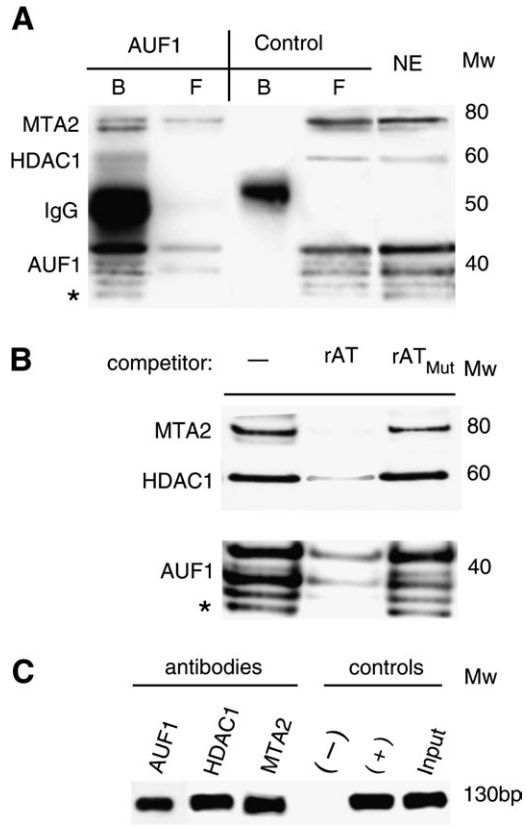

Figure 5. In vitro and in vivo interactions of AUF1 with HDAC1, MTA2, and AT-rich DNA. Nuclear extracts (NE) were prepared from the E18 rat cortex and immunoprecipitated with either AUF1 or control antibody. Following immunoprecipitation, bound (B) and free (F) fractions were analyzed by Western blots using specific antibodies. The identities of AUF1-, MTA2-, and HDAC1-immunoreactive bands are marked on the left. Molecular weight (MW) is shown in kDa on the right side. Star indicates a nonspecific band (*A*). The DAPSTER assay was performed using nuclear extracts prepared from the E18 rat cortex. DNA affinity assay was either carried out in the absence of competitors (-), or in the presence of the specific competitor rAT or control rAT_{MUT} dsDNA. The presence of the AUF1, HDAC1 and MTA2 in the DNA–protein complex was determined by Western blot using specific antibodies. The identities of AUF1-, MTA2- and HDAC1-immunoreactive bands are marked on the left (*B*). A ~150-bp DNA fragment containing the rAT DNA region was amplified from samples that were immunoprecipitated with AUF1, HDAC1 or MTA2 antibodies and PCR amplicons were separated on agarose gels. No DNA was amplified from samples that were immunoprecipitated using the preimmune serum to AUF1 or a control antibody (EGFR). The ChIP assay was performed on postnatal (P2) rat cortical tissue. Precipitated DNA fragments were amplified by PCR, then the product of the nested (2nd) PCR was subjected to agarose gel electrophoresis and DNA fragments were visualized by ethydium bromide staining under UV light. Input sample indicates the nonimmunoprecipitated positive control; plasmid DNA containing the rAT region used as template for PCR amplification was used as another positive control (+). For the negative control (-) we used the EGFR-precipitated sample (*C*).

assay enabling the identification of proteins that specifically bind to the test DNA sequences (Kumar and Bernstein 2001). For the DAPSTER assay, we immobilized the same AT-rich dsDNA that we used to isolate AUF1 from the developing rodent cortex (Dobi et al. 2006) and performed the assay using nuclear extracts isolated from the P2 cortex that were preincubated with specific (rAT) or nonspecific (rAT_{MUT}) oligonucleotides. As a positive control, we also performed this DNA affinity purification without competing DNA. Western analysis of the bound and free fractions showed that in addition to AUF1, both HDAC1 and MTA2 were present in the DNA–protein complex when no competitor or the nonspecific competitor was present (Fig. 5*B*). Because neither HDAC1 nor MTA2 possess DNA-binding domains (Zhang et al. 1999 Yao and Yang 2003) their presence in the AT-rich dsDNA-binding complex was likely mediated through AUF1. The formation of the AT-rich dsDNA–protein complex was specific because preincubation of nuclear extracts with excess AT-rich dsDNA (rAT) used as a specific competitor almost completely abolished the binding of all proteins. Preincubation of the nuclear extracts with the nonspecific/control competitor dsDNA (rAT_{MUT}) on the other hand did not significantly affect the formation of the complex.

We performed the chromatin immunoprecipitation (ChIP) assay to test whether the demonstrated in vitro interactions between AT-rich dsDNA and the 3 proteins also take place in vivo. For the ChIP assay, we used microdissected cortices from P2 rats because all 3 proteins were still expressed and the P2 cortex yielded sufficient cortical tissue required for the cross-linking studies (Dobi et al. 2006). Following PF cross-linking, we incubated the cortical samples with anti-AUF1, anti-HDAC1, anti-MTA2 antibodies, or a negative control antibody. Following multiple washing steps, we isolated DNA from immunoprecipitated samples and used it as a template in PCR along with primers that flank the AT-rich dsDNA element (Dobi et al. 2006). Our results showed that the AT-rich DNA region could be amplified from the samples precipitated with AUF1, HDAC1 as well as MTA2 antibodies but not with the control antibody (Fig. 5*C*). These results demonstrated that AUF1, HDAC1, and MTA2 were all associated with the AT-rich DNA element in vivo and implicating AUF1 in recruiting both HDAC1 and MTA2 to AT-rich DNA regions.

Altering Histone Acetylation Modulates the Effect of AUF1 on Gene Expression

As a 1st step toward identifying the potential role of the detected interactions between AT-rich dsDNA, AUF1, HDAC1, and MTA2 in regulating gene expression, we used MEF-$AUF1^{-/-}$ and MEF-$AUF1^{+/+}$ cells for our transient transfection analysis. We selected these cells for our initial studies because the cultures were composed of identical population of embryonic primary cells that differ only in the presence of AUF1, they can be transfected with high efficiency and they endogenously express HDAC1 and MTA2. The presence of AUF1 decreased reporter gene expression by approximately 50% and TSA treatment of these cells caused a substantial increase in reporter gene activity (Fig. 6). Importantly, mutant cells lacking AUF1 (MEF-$AUF1^{-/-}$) showed no response to TSA treatment. TSA treatment had no effect on reporter gene activities when MEF-$AUF1^{+/+}$ and MEF-$AUF1^{-/-}$ cell cultures were transfected with the control reporter plasmid TK-rAT_{mut}–Ren. These results suggested that the molecular function of AUF1 depends on its specific binding to the AT-rich DNA site and involves directing the effect of histone acetylation or deacetylation to these AT-rich DNA elements.

Absence of AUF1 Alters the Composition of the NuRD Complex

To understand the molecular mechanism of AUF1 function in vivo, we analyzed the effect of lack of AUF1 on the composition of the NURD complex in the developing brain. Using semi-quantitative ChIP assay, we compared the relative amounts of HDAC1 and MTA2 associated with the AT-rich DNA in the

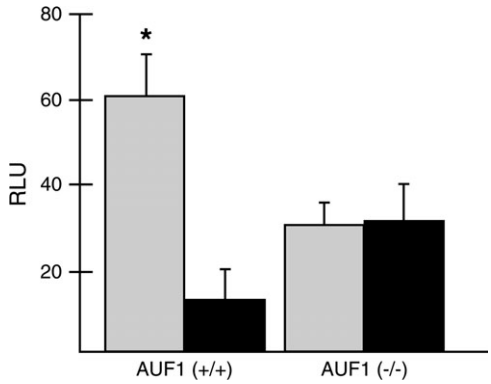

Figure 6. The effect of TSA treatment on AUF1-dependent reporter gene activity. MEF-AUF1$^{+/+}$ and MEF-AUF1$^{-/-}$ cells were transfected with reporter plasmids pTK-rAT-Ren or pTK-rAT$_{MUT}$-Ren and treated with TSA (gray columns) or with vehicle (black columns). The results were normalized by subtracting values measured in cultures transfected with pTK-rAT$_{MUT}$-Ren from values obtained from cultures transfected with pTK-rAT$_{MUT}$-Ren and expressed as RLU. The lack of AUF1 in MEF-AUF1$^{-/-}$ cells resulted in a significant loss of the AT-rich DNA dependent repressor of AUF1 and a loss of the effect of TSA treatment. Star = $P \leq 0.05$; $N = 4$, $\pm$SD.

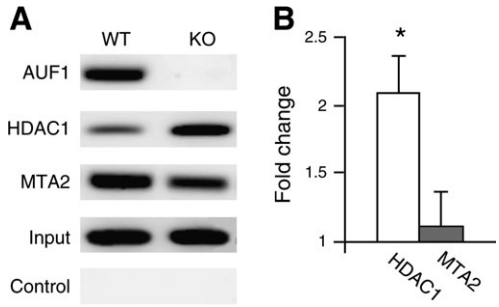

Figure 7. AUF1 proteins interact with both the mAT^{ENK} region and the NuRD complex and control chromatin remodeling. Semiquantitative ChIP assay was performed using whole brain tissue from P2 wild-type (WT) or AUF1 knockout (KO) mouse brains. A 274-bp DNA fragment containing the AT-rich regulatory region of the mouse ENK gene, or a negative control region was amplified from samples that were immunoprecipitated with anti-AUF1, anti-HDAC1, anti-SATB2 (Szemes et al. 2006), or anti-MTA2 antibodies, or normal rabbit serum as a negative control (not shown). As a negative control for AUF1-binding, we used a region in the GAPDH gene (control shown). After amplification by PCR, the product was subjected to agarose gel electrophoresis and DNA fragments were visualized by SYBR Safe staining (*A*). Images were collected using the Fuji 3000 LAS intelligent dark box equipped with a CCD camera, and band densities were quantified with the Image Gauge software. Raw values were normalized to the input and background, and then the fold change difference between KO to WT was calculated. Star = $P \leq 0.05$; $N = 4$. The average values from 3 independent experiments are shown with error bars indicating $\pm$ SD (*B*).

neonatal brains of AUF1 null mutant and wild-type animals. The primers were designed and the conditions of the PCR were adjusted enabling semiquantitative analysis (Strahl-Bolsinger et al. 1997).

We have found that in the absence of AUF1, the relative proportion of HDAC1 increased about 2-fold (Fig. 7). This increase was specific to the AT-rich DNA region because there was no difference between the wild-type and mutant animals when the GAPDH control region was amplified from samples precipitated with any of the antibodies used. Interestingly, the relative amount of MTA2 in the complex did not change significantly in the AUF1 mutant brain.

Discussion

The goal of our present study was to gain an understanding about the role of AUF1 in the developing cortex. Based on our data presented above we propose that AUF1 proteins are involved in coordinating gene expression in proliferating neuronal precursors/progenitors and differentiating cortical neurons by recruiting chromatin remodeling molecules to AT-rich DNA elements. This is important because studies have shown that chromatin remodeling can play important roles at various stages of corticogenesis by coordinating the expression of multiple genes (Berube et al. 2005). At the molecular level, they provide permissive or restrictive chromatin environment for classical transcription factors during cellular differentiation, however, the identity of proteins directing their effect to specific genomic loci is little known (Hsieh and Gage 2005). AUF1 was recently also found to regulate DNA methyltransferase 1, an important determinant of genome-wide DNA methylation (Torrisani et al. 2007.)

We found that all AUF1 isoforms were expressed in the developing cortex and the ratio between the various isoforms did not change significantly between E14 and P2. AUF1 proteins were highly expressed in the E14 brain by proliferating cells. In addition to neural precursor/progenitor cells that were dividing by asymmetrical cell divisions (Ohnuma and Harris 2003), AUF1 may also be expressed in self-renewing neural stem cells that undergo limited cycles of symmetrical cell divisions. In the E14 brain, AUF1+ cells in the VZ express PH3, indicating that AUF1 was expressed during in the M phase of cell cycle. During M phase, inherited determinants of cell fate are localized to only 1 pole of the mother cell undergoing asymmetric cell division, thus only 1 of the daughter cells will inherit such a determinant (Bally-Cuif and Hammerschmidt 2003; Ohnuma and Harris 2003). Whether AUF1 falls into this category, that is, it is inherited by only 1 daughter cell, needs to be addressed in future experiments. Our preliminary BrdU labeling studies indicated that AUF1 was also expressed in BrdU-positive cells (see Supplementary Fig. 5). Because chromatin remodeling during S phase is thought to play a major role in regulating cellular differentiation (Ohnuma and Harris 2003) and because differentiating neurons change their fate according to their environments if they were in S (or G1) phase (McConnell 1988), AUF1 could be involved in regulating neuronal differentiation through altering the access of transcription factors to their DNA-binding sites.

Our double-immunohistochemical experiments showed an almost complete coexpression of AUF1 proteins with HDAC1 and MTA2 at a single cell level and ChIP assay demonstrated direct, simultaneous interaction between AUF1, HDAC1, MTA and the AT-rich dsDNA in vivo. Previous studies have also shown that developmental regulators such as BRG1 (Matsumoto et al. 2006) and repressor element silencing transcription factor/neuron restricture silencing factor (REST-NRSF) Ballas and Mandel 2005; Lunyak and Rosenfeld 2005 regulate fate determination of neural stem cells and/or neural differentiation through their interaction with members of the mSin3A/B chromatin remodeling complex that contains HDAC1 (as well as HDAC2) (Ahringer 2000). Another chromatin remodeling complex that contains HDAC1 is the NuRD complex (Ahringer 2000; Feng and Zhang 2003; Bowen et al. 2004. The NuRD complex regulates chromatin structure through multiple

mechanisms including histone deacetylation. Both HDAC1 and MTA2 are members of the complex and blocking histone deacetylase activity by TSA or valproic acid resulted in promoting a neuronal fate at the expense of a glial 1 (Hsieh et al. 2004; Shen et al. 2005.

Our immunohistochemical studies have shown that AUF1 remains expressed in postmitotic differentiating cortical neurons and that AUF1 was also coexpressed in these cells with HDAC1 and MTA2. These findings implicate AUF1 in regulating gene expression at different stages of neuronal lineage progression through chromatin remodeling (Recillas-Targa and Razin 2001). Accumulation of acetylated histone molecules prevents chromatin condensation and the resulting open chromatin structure permits the binding of sequence-specific transcription factors to their *cis*-regulatory DNA elements, thus resulting in increased transcription of target genes (Alvarez et al. 2000. Conversely, histone deacetylation mediated by HDACs results in a closed chromatin structure, thus preventing the binding of transcription factors to their DNA elements (Mal et al. 2001. In this study, we focused on the NuRD complex because it has been shown that the complex plays an important regulatory role in the differentiation of multiple cell types including neural cells (Feng and Zhang 2003). The complex regulates chromatin structure through multiple mechanisms that include histone deacetylation and nucleosome remodeling (Yao and Yang 2003). The complex is approximately 2 MDa in size, comprising at least 7 polypeptides that include HDAC1 and MTA2. HDAC1—along with HDAC2—is also part of the Sin3a chromatin remodeling complex (Zhang et al. 1999). Because MTA2 is not a part of the Sin3a complex (Ahringer 2000), the coexpression of HDAC1 and MTA2 in AUF1+ cortical neurons suggests that the chromatin remodeling complex is NuRD rather than Sin3a. Because hypoacetylated histone amino-termini are generally correlated with transcriptional repression (Yao and Yang 2003), recruiting the NuRD complex to AT-rich DNA by AUF1 should result in repressor activity. Indeed, using a model system we have shown that AUF1 is important in directing the effect of altered histone deacetylation, that is, closed chromatin structure to AT-rich dsDNA resulting in decreased reporter gene activity.

AT-rich DNA elements appear frequently in the genome (Woynarowski 2004). AT-rich sequences can form 3-dimensional binding sites for nuclear proteins that recognize 3-dimensional structure rather than a short nucleotide sequence (Strick and Laemmli 1995; Laemmli and Tjian 1996; Strick et al. 2000. AUF1 thus joins the family of AT-rich DNA-binding proteins that include nucleolin (Dickinson and Kohwi 1995), histone H1 (Pauli et al. 1989), HMGI/Y (Reeves 2000), SATB1 (Dickinson et al. 1992) and SATB2 (Britanova et al. 2005; Szemes et al. 2006). SATB1 is especially interesting because it interacts with and recruits members of the NuRD (and also chromatin accessibility complex and ATP-dependent chromatin assembly and remodelling factor (ACF) chromatin remodeling complexes to AT-rich DNA sites and regulates nucleosome positioning over several kilobases (Yasui et al. 2002). Previous studies showed that these AT-rich DNA-binding proteins, AUF1, SATB1, and SATB2, are expressed in a nonoverlapping fashion during cortical development and they interact with both the nuclear matrix and with chromatin remodeling complexes (Britanova et al. 2005; Dobi et al. 2006; Gyorgy et al. 2006 Szemes et al. 2006). These observations raise the intriguing possibility that there may be a development-specific modification of the chromatin structure in differentiating cortical neurons influenced by both genetic and epigenetic factors. This is important because despite the great progress made in identifying transcription factors and signaling molecules involved in regulating corticogenesis (Rakic 2006), we still lack a good understanding about the identity of molecules that integrate environmental signals and genetic programs believed to play a key role in coordinating gene expression (Jaenisch and Bird 2003). The surprising change in the relative abundance of HDAC1 in the NURD complex of AUF1 mutant animals suggests that altered abundance of the key members of the complex may alter the expression levels of downstream genes. Our preliminary microarray data analyzing the transciptome of AUF1 mutant brains indeed showed that the expression levels of genes associated with cell-adhesion and migration are altered in the mutant animals (data not shown). These molecular abnormalities may contribute to the apparent callosal dysgenesis of AUF1 mutant animals (see Supplementary Fig. 6.).

Understanding how AUF1 fits into the regulatory network of molecules that control gene expression during cortical development is currently not known. The majority of the identified transcription regulators of cortical development are classical short DNA sequence-specific binding proteins (Sommer et al. 1996 Kageyama et al. 1997; Guillemot 2005). Mutations of these genes result in specific developmental deficits. For example, in the absence of Dlx1/Dlx2, the "master" regulators of telencephalic development, the regionalization of the telencephalon is abnormal and there is a deficit in a subset of cortical interneurons (Cobos et al. 2005. Whether AUF1 acts up or downstream from Dlx and other classical regulators of cortical development is currently unknown. Because knockout animals, including Dlx1/2 double mutants are available (Cobos et al. 2005), experiments can be designed to address this important issue. Additional studies will be also needed to identify which one(s) of the multiple molecular regulatory functions of AUF1, regulating mRNA stability (Brewer 2002), gene transcription (Dobi et al. 2006) and chromatin remodeling (this paper) is/are required during corticogenesis.

Supplementary Material

Supplementary material can be found at: http://www.cercor.oxfordjournals.org/.

Funding

USUHS Intramural grant; and National Institute of Child Health and Human Development grant

Notes

We thank Dr Jozsef Czege for his expert help during the imaging studies. *Conflict of Interest*: None declared

Address correspondence to Dr Denes V. Agoston, APG, USUHS, 4301 Jones Br Rd. Bethesda, MD 20814, USA. Email: vagoston@usuhs.edu.

References

Ahringer J. 2000. NuRD and SIN3 histone deacetylase complexes in development. Trends Genet. 16:351–356.

Alvarez JD, Yasui DH, Niida H, Joh T, Loh DY, Kohwi-Shigematsu T. 2000. The MAR-binding protein SATB1 orchestrates temporal and

spatial expression of multiple genes during T-cell development. Genes Dev. 14:521–535.
Ballas N, Mandel G. 2005. The many faces of REST oversee epigenetic programming of neuronal genes. Curr Opin Neurobiol. 15:500–506.
Berube NG, Mangelsdorf M, Jagla M, Vanderluit J, Garrick D, Gibbons RJ, Higgs DR, Slack RS, Picketts DJ. 2005. The chromatin-remodeling protein ATRX is critical for neuronal survival during corticogenesis. J Clin Invest. 115:258–267.
Blaxall BC, Dwyer-Nield LD, Bauer AK, Bohlmeyer TJ, Malkinson AM, Port JD. 2000. Differential expression and localization of the mRNA binding proteins, AU-rich element mRNA binding protein (AUF1) and Hu antigen R (HuR), in neoplastic lung tissue. Mol Carcinog. 28:76–83.
Brenner RM, Slayden OD, Rodgers WH, Critchley HO, Carroll R, Nie XJ, Mah K. 2003. Immunocytochemical assessment of mitotic activity with an antibody to phosphorylated histone H3 in the macaque and human endometrium. Human reproduction. 18(6): 1185–1193.
Britanova O, Akopov S, Lukyanov S, Gruss P, Tarabykin V. 2005. Novel transcription factor Satb2 interacts with matrix attachment region DNA elements in a tissue-spacific manner and demonstrates cell-type-dependent expression in the developing mouse CNS. Eur J Neurosci. 21:658–668.
Brewer G. 2002. Messenger RNA decay during aging and development. Ageing Res Rev. 1:607–625.
Bowen NJ, Fujita N, Kajita M, Wade PA. 2004. Mi-2/NuRD: multiple complexes for many purposes. Biochim Biophys Acta. 1677: 52–57.
Cobos I, Calcagnotto ME, Vilaythong AJ, Thwin MT, Noebels JL, Baraban SC, Rubenstein JL. 2005. Mice lacking Dlx1 show subtype-specific loss of interneurons, reduced inhibition and epilepsy. Nat Neurosci. 8:1059–1068.
Dempsey LA, Hanakahi LA, Maizels N. 1998. A specific isoform of hnRNP D interacts with DNA in the LR1 heterodimer: canonical RNA binding motifs in a sequence-specific duplex DNA binding protein. J Biol Chem. 273:29224–29229.
Dickinson LA, Joh T, Kohwi Y, Kohwi-Shigematsu T. 1992. A tissue-specific MAR/SAR DNA-binding protein with unusual binding site recognition. Cell. 70:631–645.
Dickinson LA, Kohwi ST. 1995. Nucleolin is a matrix attachment region DNA-binding protein that specifically recognizes a region with high base-unpairing potential. Mol Cell Biol. 15:456–465.
Dobi A, Szemes M, Lee C, Palkovits M, Lim F, Gyorgy A, Mahan MA, Agoston DV. 2006. AUF1 is expressed in the developing brain, binds to AT-rich double-stranded DNA, and regulates enkephalin gene expression. J Biol Chem. 281:28889–28900.
Enokizono Y, Konishi Y, Nagata K, Ouhashi K, Uesugi S, Ishikawa F, Katahira M. 2005. Structure of hnRNP D complexed with single-stranded telomere DNA and unfolding of the quadruplex by hnRNP D. J Biol Chem.
Eversole A, Maizels N. 2000. In vitro properties of the conserved mammalian protein hnRNP D suggest a role in telomere maintenance. Mol Cell Biol. 20:5425–5432.
Feng Q, Zhang Y. 2003. The NuRD complex: linking histone modification to nucleosome remodeling. Curr Top Microbiol Immunol. 274:269–290.
Guillemot F. 2005. Cellular and molecular control of neurogenesis in the mammalian tlencephalon. Curr Opin Cell Biol. 17:639–647.
Gyorgy AB, Szemes M, de Juan Romero C, Tarabykin V, Agoston DV. 2008. SATB2 interacts with chromatin-remodeling molecules in differentiating cortical neurons. Eur J Neurosci. 27:865–873.
Hsieh J, Gage FH. 2004. Epigenetic control of neural stem cell fate. Curr Opin Genet Dev. 14:461–469.
Hsieh J, Gage FH. 2005. Chromatin remodeling in neural development and plasticity. Curr Opin Cell Biol. 17:664–671.
Jaenisch R, Bird A. 2003. Epigenetic regulation of gene expression: how the genome integrates intrinsic and environmental signals. Nat Genet. 33(Suppl.):245–254.
Kageyama R, Ishibashi M, Takebayashi K, Tomita K. 1997. bHLH transcription factors and mammalian neuronal differentiation. Int J Biochem Cell Biol. 29:1389–1399.
Kim JH, Panchision D, Kittappa R, McKay R. 2003. Generating CNS neurons from embryonic, fetal, and adult stem cells. Methods Enzymol. 365:303–327.
Kumar NV, Bernstein LR. 2001. A new analytical scale DNA affinity binding assay for analyses of specific protein-DNA interactions. Anal Biochem. 299:203–210.
Laroia G, Schneider RJ. 2002. Alternate exon insertion controls selective ubiquitination and degradation of different AUF1 protein isoforms. Nucleic Acids Res. 30:3052–3058.
Lu JY, Sadri N, Schneider RJ. 2006. Endotoxic shock in AUF1 knockout mice mediated by failure to degrade proinflammatory cytokine mRNAs. Genes Dev. 20:3174–3184.
Lu JY, Schneider RJ. 2004. Tissue distribution of AU-rich mRNA-binding proteins involved in regulation of mRNA decay. J Biol Chem. 279:12974–12979.
Lunyak VV, Rosenfield MG. 2005. No rest for REST: REST/NRSF regulation of neurogenesis. Cell. 121:499–501.
Mal A, Sturniolo M, Schiltz RL, Ghosh MK, Harter ML. 2001. A role for histone deacetylase HDAC1 in modulating the transcriptional activity of MyoD: inhibition of the myogenic program. Embo J. 20:1739–1753.
Maric D, Maric I, Chang YH, Barker JL. 2003. Prospective cell sorting of embryonic rat neural stem cells and neuronal and glial progenitors reveals selective effects of basic fibroblast growth factor and epidermal growth factor on self-renewal and differentiation. J Neurosci. 23:240–251.
McConnell SK. 1988. Fates of visual cortical neurons in the ferret after isochronic and heterochronic transplantation. J Neurosci. 8:945–974.
Ohnuma S, Harris WA. 2003. Neurogenesis and the cell cycle. Neuron. 40:199–208.
Pauli U, Chiu JF, Ditullio P, Kroeger P, Shalhoub V, Rowe T, Stein G, Stein J. 1989. Specific interactions of histone H1 and a 45 kilodalton nuclear protein with a putative matrix attachment site in the distal promoter region of a cell cycle-regulated human histone gene. J Cell Physiol. 139:320–328.
Rakic P. 2006. A century of progress in corticoneurogenesis: from silver impregnation to genetic engineering. Cereb Cortex. 16(Suppl. 1):i3–i17.
Rayzman VM, Sentry JW. 2006. MCA1 detection of histone H3 serine 10 phosphorylation, a noverl biomarker for determination of mitotic indices. Human antibodies. 15:71–80.
Recillas-Targa F, Razin SV. 2001. Chromatin domains and regulation of gene expression: familiar and enigmatic clusters of chicken globin genes. Crit Rev Eukaryot Gene Expr. 11:227–242.
Reeves R. 2000. Structure and function of the HMGI(Y) family of architectural transcription factors. Environ Health Perspect. 108:803–809.
Sarkar B, Xi Q, He C, Schneider RJ. 2003. Selective degradation of AU-rich mRNAs promoted by the p37 AUF1 protein isoform. Mol Cell Biol. 23:6685–6693.
Shen S, Li J, Casaccia-Bonnefil P. 2005. Histone modifications affect timing of oligodendrocyte progenitor differentiation in the developing rat brain. J Cell Biol. 169:577–589.
Sommer L, Ma Q, Anderson DJ. 1996. Neurogenins, a novel family of atonal-related bHLH transcription factors, are putative mammalian neuronal determination genes that reveal progenitor cell heterogeneity in the developing CNS and PNS. Mol Cell Neurosci. 8:221–241.
Strahl-Bolsinger S, Hecht A, Luo K, Grunstein M. 1997. SIR2 and SIR4 interactions differ in core and extended telomeric heterochromatin in yeast. Genes Dev. 11:83–93.
Szemes M, Gyorgy A, Paweletz C, Dobi A, Agoston DV. 2006. Isolation and characterization of SATB2, a novel AT-rich DNA binding protein expressed in development- and cell-specific manner in the rat brain. Neurochem Res. 31:643–655.
Tolnay M, Baranyi L, Tsokos GC. 2000. Heterogeneous nuclear ribonucleoprotein D0 contains transactivator and DNA-binding domains. Biochem J. 348(Pt 1):151–158.
Torrisani J, Unterberger A, Tendulkar SR, Shikimi K, Szyf M. 2007. AUF1 cell cycle variations define genomic DNA methylation by regulation of DNMT1 mRNA stability. Mol Cell Biol. 1:395–410.
Wagner BJ, DeMaria CT, Sun Y, Wilson GM, Brewer G. 1998. Structure and genomic organization of the human AUF1 gene: alternative pre-Mrna splicing generates four protein isoforms. Genomics. 48:195–202.

Woynarowski JM. 2004. AT islands—their nature and potential for anticancer strategies. Curr Cancer Drug Targets. 4:219–234.
Yao YL, Yang WM. 2003. The metastasis-associated proteins 1 and 2 form distinct protein complexes with histone deacetylase activity. J Biol Chem. 278:42560–42568.
Yasui D, Miyano M, Cai S, Varga-Weisz P, Kohwi-Shigematsu T. 2002. SATB1 targets chromatin remodelling to regulate genes over long distances. Nature. 419:641–645.
Zhang Y, Ng HH, Erdjument-Bromage H, Tempst P, Bird A, Reinberg D. 1999. Analysis of the NuRD subunits reveals a histone deacetylase core complex and a connection with DNA methylation. Genes Dev. 13:1924–1935.
Zhang W, Wagner BJ, Ehrenman K, Schaefer AW, DeMaria CT, Crater D, DeHaven K, Long L, Brewer G. 1993. Purification, characterization, and cDNA cloning of an AU-rich element RNA-binding protein, AUF1. Mol Cell Biol. 13:7652–7665.